DEUTSCHES ELEKTRONEN-SYNCHROTRON DESY

DESY SR 84-10
April 1984

ELECTRONIC STRUCTURE OF SOLID PYRIDINE AND PYRIDINE ADSORBED ON POLYCRYSTALLINE SILVER

by

J.-H. Fock, J. Schmidt-May

II. Institut f. Experimentalphysik, Universität Hamburg

E.E. Koch

Hamburger Synchrotronstrahlungslabor HASYLAB at DESY

ISSN 0723-7979

NOTKESTRASSE 85 · 2 HAMBURG 52

DESY SR 84-10
April 1984

ISSN 0723 - 7979

Electronic Structure of Solid Pyridine and Pyridine Adsorbed on Polycrystalline Silver [*]

J.-H. Fock[#] and J. Schmidt-May
II. Institut für Experimentalphysik, Universität Hamburg
D-2000 Hamburg 50, Germany

and

E.E. Koch
Hamburger Synchrotronstrahlungslabor HASYLAB at DESY
D-2000 Hamburg 52, Germany

Abstract

The electronic structure of the valence bands of polycrystalline films of pyridine (C_5H_5N) including all valence levels extending from initial energies of 4 eV down to 30 eV ($E_{VAC} = 0$) has been determined from photoelectron energy distribution measurements for photon energies 20 eV $\leq h\nu \leq$ 170 eV using synchrotron radiation. The valence bands showing a one to one correspondence to the gas phase, a rigid relaxation shift of $\Delta E_R = 0.3$ eV for the vertical binding energies and a considerable solid state broadening ($\gtrsim 0.5$ eV) are assigned in comparison to recent MO-calculations. By tuning the photon energy and thereby achieving high surface sensitivity for $h\nu$ around 45 eV we have also studied pyridine adsorbed at 120 K (6 Langmuir) on in situ prepared polycrystalline Ag-substrates. Thus we were able to study in detail the surface electronic structure in the range of the Ag 4d bands. Due to a strong mixing of substrate 4d and pyridine $2b_1(\pi)$, $1a_2(\pi)$ and $7a_1(n)$ energy levels the surface electronic structure gets strongly modified in the upper part of the 4d bands and a strong and sharp (0.4 eV FWHM) surface resonance at an energy of 3.7 eV below E_F^{Ag} is observed which we attribute to a 4d-$7a_1(n)$ bonding of the nitrogen lone pair orbital.

[*] Work supported in part by Bundesministerium für Forschung und Technologie (BMFT) from funds for research with synchrotron radiation

[#] now at: Max-Planck-Institut für Festkörperforschung, Heisenbergstr. 1, D-7000 Stuttgart 80, Germany

---

submitted to: J. Electr. Spectr. and Rel. Phen.

Introduction

Organic molecules in the condensed solid phase form molecular crystals with weak van der Waals forces between the individual molecules constituting the crystal and in general the free molecular electronic structure largely determines the electronic structure of the crystal. This view has now been supported by a large number of photoemission experiments for monomolecular organic solids [1]. A different situation is encountered for thin films or adsorbates of organic molecules on metal surfaces, where a strong substrate-adsorbate interaction may be observed [2]. While no detailed study of the electronic structure of solid pyridine is available several photoemission studies for pyridine adsorbed on metal surfaces have recently been reported (e.g. Ref. 3-12). These experiments include UPS studies of the valence band region both in angle integrated [e.g. 8-10] and angle resolved modes e.g. [3-7,11] as well as XPS carbon 1s and nitrogen 1s studies [10,12]. An obvious difficulty in these studies is the strong overlap of the high lying pyridine $1a_2(\pi)$, $2b_1(\pi)$ and $7a_1(n)$ molecular orbitals (MO's) with the metal valence bands which leads to difficulties in resolving the structures with certainty.

In particular for silver there is an almost perfect overlap with the Ag 4d bands and hence mostly lower lying MO's (having larger binding energies) of chemisorbed pyridine have been discussed [9,10]. On the other hand the adsorption of pyridine on nobel metal surfaces such as Ag, Cu and Au is of particular interest in connection with surface-enhanced Raman scattering (SERS) [13] and information concerning the uppermost orbitals of adsorbed pyridine is quite important in discussing the SERS-mechanism [14].

In the present paper we start our discussion by presenting photoemission results for condensed *solid pyridine*. By comparing our results to gas phase spectra [15,16] and to recent MO calculations [17-20] we obtain an assignment for the valence band features in the energy distribution curves. We show that most calculations although they give the right "bunching" of orbitals fail to predict the correct binding energies for the whole valence band region.

For *pyridine adsorbed at 120 K* on polycrystalline Ag substrates we observe similar to the solid phase little differences to the free molecule behaviour for pyridine derived bands with binding energies $E_B \geq 7$ eV ($E_F^{Ag} = 0$). However, for the uppermost π orbitals $1a_2$ and $2b_1$ and the lone pair nitrogen $7a_1$ MO which strongly overlap with the top of the Ag 4d bands the electronic structure gets strongly modified and a sharp surface resonance (FWHM 0.4 eV) at the Ag 4d band edge is observed at 3.7 eV below the Fermi energy. This means that presumably for the low temperature pyridine adsorption, where the molecule has been shown to be N bonding to the substrate [9,10,21], the molecule forms a chemical bond involving electronic Ag 4d states at the surface. This view is supported by our recent observation of surface induced local d-band states in the upper 4d band between ~ 4 and 5.2 eV below E_F for clean poylcrystalline silver films [22].

Experiment

The experiments were performed in the synchrotron radiation laboratory HASYLAB at the 5 GeV DORIS II storage ring at DESY, Hamburg. Angle integrated photoelectron energy distribution curves (EDC's) were measured with a commercial double-pass cylindrical mirror analyzer (CMA) with the use of the FLIPPER monochromator [23] for excitation energies ranging from $h\nu = 20$ eV up to 170 eV. The overall resolution (monochromator and electron analyzer) for the pyridine valence bands was between 1.2 eV at $h\nu = 170$ eV and 0.3 eV at $h\nu = 20$ eV, which was sufficient for an accurate determination of EDC features which have typical widths of 1.0 - 2.0 eV (FWHM). The Ag films were evaporated in situ onto stainless steel substrates under UHV conditions at room temperature, with a base pressure below 2×10^{-10} torr and about 5×10^{-10} torr during evaporation. The cryodeposited pyridine films were evaporated on the metal surface cooled to liquid nitrogen temperature (~ 120 K) using a small gas inlet tube in close proximity to the surface. In order to avoid charging problems during photoemission the sample thickness was limited to roughly 10 nm for the studies of solid pyridine. For the Ag/pyridine adsorption experiments exposures of the cooled Ag surface of about 6 L (1 L = 10^{-6} torr sec), were performed.Ion gauge readings were divided by a factor of 5.8 [9].

Results and Discussion

A) Bulk Solid Pyridine

In Fig. 1 we show the photoelectron energy distribution curves for solid pyridine for three photon energies of the exciting light. Initial energies are referred to the vacuum level ($E_{VAC} = 0$) of the silver substrate assuming a work function of $\Phi^{Ag} = 4.3$ eV for silver. Five groups of bands labeled A to E canbe distinguished in the binding energy range down to 30 eV. The group B extending from 11 eV down to 18 eV consist at least of two peaks and a shoulder the shape of which varies slightly with photon energy. The upper part of the valence bands is in agreement with previous measurements [8,9]. While the shape of the spectra shows slight variations with photon energy we observe a remarkable increase of the relative intensities of the maxima C, D and E (and part of B) with respect to peak A with increasing photon energy. Thus for instance the intensity ratio I_A/I_C changes from 1.4 to 0.85 when the photon energy is raised from 70 eV to 170 eV. This observation is in agreement with expectations for the photon energy dependence of s-like versus p or π atomic or molecular cross sections, where the partial p- (or π) type cross sections are known to fall faster with increasing energy than the s-type partial cross sections [24]. This behaviour identifies the maxima C, D and E immediately as derived mainly from carbon and nitrogen 2s MO's.

In Fig. 2 we compare the upper part of the valence band with a photoelectron spectrum for gaseous pyridine [16]. The gas phase spectrum has been shifted by the solid state relaxation energy $\Delta E_R = 0.3$ eV in the figure in order to align it with its solid phase analogue. In this way a clear one-to-one correspondence of the main features in the solid state to the gas phase spectrum emerges, which is typical for monomolecular van der Waals solids [1]. Thus it is easy to assign the peaks for solid pyridine. The binding energies of the valence bands together with the assignments are collected in table 1 where also the gas phase results [16] are given for comparison. The resulting gas-to-solid shifts are 0.3 eV for the vertical ionization potentials. The adiabatic ionization potential of the uppermost valence orbital is lowered by 1.3 eV compared to the gas phase.

A feature of the solid spectrum immediately obvious from Fig. 2 is the considerable broadening in the order of 0.5 eV to 1.0 eV of the peaks with respect to the gas phase. Thus the individual bands contributing to peak A and the structured band B can no longer be seperated. This broadening is related to the relaxation shift [25,26]. Following the detailed model and discussion given by Duke et al. [25] we note that the net shift arises from the polarization of the surrounding molecules by the charge localized on the molecular cation. A large temperature independent contribution to the widths in the solid state is generated primarily by spatial inhomogeneities in the local environment of the cations in the bulk, at the surface and at grain boundaries. These local variations cause fluctuations in the intermolecular relaxation energies. The E($\underline{k}$) dispersions in molecular crystals which in a polycrystalline sample would also lead to a broadening are in comparison with the magnitude of the broadening mechanism described above, roughly an order of magnitude smaller (0.1 eV to 0.2 eV) because of the weak van der Waals interaction and small wavefunction overlap between adjacent molecules.

In Fig. 3 we present a synopsis of some MO calculations for pyridine which guided us in the assignment of the EDC's. Without going into a detailed comparison with experiment we wish to point out a few major points: (i) Most calculations agree in the rough ordering of the MO's, in particular in the bunching of groups of orbitals. (ii) There is no calculation which describes simultaneously the whole valence band region satisfactory, except for the semiempirical calculation by Almlöf et al. [19].(iii) The ordering of the uppermost three orbitals including two π- and the nitrogen lone pair n-orbital is at variance between different calculations. We assumed for table 1 the ordering which was recently also adopted for the interpretation of the high resolution gas phase spectrum [16] . Of course with accompanying vibrational progressions there is considerable overlap between the uppermost two bands.

B) Pyridine Adsorbed on Polycrystalline Silver

As mentioned above the system pyridine/Ag has played a major role in the recent discussion of the SERS-mechanism [13,14]. Yet the detailed structure of the uppermost MO's of pyridine adsorbed on Ag and the study of the interaction with the substrate 4d bands has largely escaped experimental observation. In the present experiment the surface sensitivity was tuned by variation of the photon energy. The escape depth Λ for Ag has only been determined for a few kinetic energies (Λ^{7eV} = 38 Å, Λ^{75eV} = 4 Å, Λ^{350eV} = 8 Å) [27]. Nevertheless, it is clear that it has its minimum below 100 eV kinetic energy with only few Å and hence experiments in this range are extremely surface sensitive. In fact our recent results for clean silver surfaces [22] suggested an optimum surface sensitivity for hν around 45 eV. For organic films a similar behaviour is expected (see e.g. [1,28]) and hence photoemission experiments with hν ≈ 45 eV are highly surface sensitive.

In Fig. 4 the results are shown for a clean silver surface and for a thin (6 L) layer of pyridine adsorbed and measured at 120 K. The energy scale is referenced to $E_F^{Ag} = 0$. In the upper part we show the measured spectra, while the difference curve is shown in the lower part together with a spectrum for solid pyridine.

Within our experimental accuracy we see no change in the upper part of the 5s bands of silver upon adsorption. The upper edge of the 4d bands is markedly changed in that a distinct shoulder can be seen (marked S in Fig. 4). Strong variations in the 4d bands are followed by features at larger binding energies ($E_B \gtrsim 7$ eV) which closely resemble the gas phase or the solid phase pyridine spectra. In the range B (between ~ 7 eV and 13.5 eV) the features induced by the adsorbed pyridine are slightly more structured than in the solid phase. The largest changes occur however at the upper edge of the 4d band in the range A of the pyridine $2b_1(\pi)$, $1a_2(\pi)$ and $7a_1(n)$ energy levels. The shoulder in the adsorbate spectrum shows up as a prominent peak in the difference spectrum centered at 3.7 eV below E_F and only ~ 0.4 eV wide. A qualitative similar absorption has already been reported in Ref. [8]. We note that other normalizations and reasonable procedures to produce the difference curve give essentially the same result as can already be judged by the appearence of the distinct shoulder in the EDC for the adsorbate. The photoemission in the top part of the 4d bands is attenuated causing the minimum in the difference curve around 4.2 eV. In this part of the Ag 4d bands surface induced local d band resonances associated with defect sites at the surface (e.g. adatoms at steps) have been identified recently [22] (since these states are degenerated with bulk 4d bands and are not expected to show dispersion we refer to these states as resonances rather than surface states).

We tentatively assign the sharp resonance to the shifted $7a_1(n)$ orbital which takes part in a weak chemical bond of pyridine with the Ag surface. This situation is depicted in Fig. 5 where we show an energy level diagram with the metallic density of states N(E) [22] and the filled orbitals of gaseous [16] and adsorbed pyridine as obtained from photoemission experiments. The Fermi level of the metal E_F and the highest occupied orbital of gaseous pyridine have been aligned in energy using the work function of clean silver Φ_{Ag} = 4.3 eV. In this way the relative shift of the $7a_1(n)$ orbital for pyridine on silver with respect to the $2b_1$ and $1a_2\pi$ -orbitals finds a natural explanation. The chemisorption band apparantly involves the local Ag 4d band surface states since they are heavily quenched whereas the remainder of the 4d band is only little affected.

Our view is corroborated by the recent temperature dependent XPS and UPS experiments for pyridine on polycrystalline Ag by Inoue et al [10] who also find for low temperatures a dominant N-bonding. We also mention similar recent experiments by Eberhardt and Plummer for CO on Ni [29] where the weak chemical bond of CO on Cu(111) involves the Λ_1 Cu surface state. We anticipate that angle resolved EDC's as well as experiments with differently prepared Ag-substrates will further clarify the situation.

Acknowledgements

This work has been supported by the Bundesministerium für Forschung und Technologie (BMFT) from funds for synchrotron radiation research. The continuous support of the HASYLAB technical staff is gratefully acknowledged. We wish to thank F. Gerken for his help in the early stage of the experiment.

References

1 see e.g. W.D. Grobman and E.E.Koch, in: Photoemission in Solids Vol. II, L. Ley and M. Cardona (editors), Springer Verlag, Heidelberg, Berlin, New York 1979, p. 261; W.R. Salaneck, in: Photon, Electron and Ion Probes of Polymer Structure and Properties, D.W. Dwight, T.J. Fabish and H.R. Thomas (editors), ACS Symposium Series Vol. 162, Am. Chem. Soc. Washington DC 1981, p. 121; L.B. Duke, in: Festkörperprobleme, Vol. 22, J. Treusch (editor), Vieweg, Braunschweig 1982, p. 21

2 see e.g. E.W. Plummer and W. Eberhardt, Adv. Chem. Phys. 49, 533 (1982); N.V. Richardson and A.M. Bradshaw, in: Electron Spectroscopy Vol. 4, C.R. Brundle and A.D. Baker (editors), Academic Press, New York 1982, ch. 3

3 D.R. Lloyd, C.M. Quinn and N.V. Richardson, Solid State Commun. 23, 141 (1977)

4 G.L. Nyberg and N.V. Richardson, Surface Science 85, 335 (1979)

5 P. Hofmann, K. Horn and A.M. Bradshaw, Surface Science 105, L260 (1981)

6 B.J. Bandy, D.R. Lloyd and N.V. Richardson, Surface Science 89, 344 (1979)

7 G.L. Nyberg, Surface Science 95, L273 (1980)

8 S.R. Kelemen and A. Kaldor, Chem. Phys. Letters 73, 205 (1980)

9 J.E. Demuth, K. Christmann and P.N. Sanda, Chem. Phys. Lett. 76, 201 (1980)

10 Y. Inoue, K. Kishi and S. Ikeda, J. Electron Spectr. and Related Phenom. 31, 109 (1983)

11 F.P. Netzer and J.-U. Mack, Chem. Phys. Lett. 95, 492 (1983)

12 G.L. Eesley and J.M. Burkstrand, Phys. Rev. B24, 582 (1981)

13 see e.g. R.K. Chang and T.E. Furtak (editors), Surface enhanced Raman scattering, Plenum Press, New York 1982; R. Dornhaus, in: Festkörperprobleme, Vol. 22, J. Treusch (editor), Vieweg, Braunschweig 1982, p. 211

14 see e.g. A. Otto, in: Light Scattering in Solids, Vol. III, M. Cardona G. Güntherodt (editors), Springer Verlag, Heidelberg, Berlin, New York 1983

15 K. Kimura, S. Kasamatu, Y. Achiba, T. Yamasaki and S. Iwata, Handbook of HeI photoelectron spectra of fundamental organic molecules, Jap. Scientific Soc. Press, Tokyo 1981

16 I. Reineck, R. Maripen, H. Veenhuizen, L. Karlsson, K. Siegbahn, M.S. Powar, Wu Nian Zu, Ji Ming Rong and S.H. Al-Shamma, J. Electr. Spectroscopy and Relat. Phenomena 27, 15 (1982)

17 D.A. Case, M. Cook and M. Karplus, J. Chem. Phys. 73, 3294 (1980)

18 W. von Niessen, W.P. Kraemer and G.H.F. Dierksen, Chem. Phys. 41, 113 (1979); see also W. von Niessen, G.H.F. Dierksen and L.S. Cederbaum, Chem. Phys. 10, 345 (1975)

19 J. Almlöf, B. Roos, U. Wahlgreen and H. Johansen, J. Electr. Spectroscopy and Relat. Phenomena 2, 51 (1973)

20 J.D. Petke, J.L. Whitten and J.A. Ryan, J. Chem. Phys. 48, 953 (1967)

21 A.L. Johnson, E.L. Muetterties and J. Stöhr, J. Am. Chem. Soc., in press, preprint Oct. 1983

22 E.E. Koch, J. Barth, J.-H. Fock, A. Goldmann and A. Otto, Solid State Commun. 42, 897 (1982)

23 J. Barth, F. Gerken, C. Kunz and J. Schmidt-May, Nucl. Instr. Methods in Physics Research 208, 307 (1983)

24 see e.g. V.I. Nefedov, N.P. Sergushin, I.M. Band and M.B. Trzhuskovskaya, J. Electr. Spectroscopy and Relat. Phenomena 2, 383 (1973)

25 C.B. Duke, W.R. Salaneck, T.J. Fabish, J.J. Ritsko, H.R. Thomas and A. Paton, Phys. Rev. B 18, 5717 (1978)

26 W.R. Salaneck, C.B. Duke, W. Eberhardt, E.W. Plummer, Phys. Rev. Letters 45, 280 (1980)

27 P.W. Palmberg and T.N. Rhodin, J. Appl. Phys. 39, 2427 (1968); H. Kanter, Phys. Rev. B1, 552 (1970); M.P. Seah, Surf. Sci. 32, 703 (1972)

28 M.P. Seah and W.A. Dench, Surface Interface Anal. 1, 2 (1979)

29 W. Eberhardt and W.E. Plummer, Phys. Rev. B28, 3605 (1983)

Table 1

Valence molecular orbital structure of gaseous (Ref. 16) and solid pyridine (this work) and assignments of the MO symmetry in C_{2v} symmetry. Comparison is also made to a recent MO calculation (Ref. 18). All energies are vertical binding energies and are given in eV referred to the vacuum level of the Ag-substrate. A work function of $\Phi = 4.3$ eV has been used for Ag.

	EXPERIMENT				MO CALCULATION
Assignment	Gas Ref. [16]	Adsorbed this work	Solid this work		Ref. [18]
$7a_1(n)$	9.66	8.0	9.6	A	9.59
$1a_2(\pi)$	9.85	9.9			9.57
$2b_1(\pi)$	10.51				10.24
$5b_2$	12.454	12.3		B	12.87
$1b_1(\pi)$	13.2				13.43
$6a_1$	13.8	13.7			14.18
$4b_2$	14.5				15.11
$5a_1$	15.838	15.4	15.3		16.32
$3b_2$					16.31 and 16.05
$4a_1$	17.1	16.8	16.8		17.94 and 18.40
$3a_1$		19.4	19.4	C	21.32 and 21.16
$2b_2$					21.29
$1b_2$		23.5	23.5	D	26.1 and 26.2[a)]
$2a_1$					27.50[a)]
$1a_1$		27.8	27.8	E	32.3[a)]

[a)] Values are taken from a figure in Ref. 18.

Figure Captions

Figure 1 Angle integrated photoelectron energy distribution curves for polycrystalline solid pyridine at 120 K for photon energies 70, 140 and 170 eV. Note the change of relative intensities of the upper valence band (e.g. peak A) relative to the lower valence band peaks (e.g. peak C) with increasing photon energy.

Figure 2 Comparison of the gas phase HeI photoelectron spectrum Ref. [16] to the EDC for solid pyridine. The gas phase spectrum has been shifted by $\Delta E_R = 0.3$ eV in order to align the main peaks. For the symmetry assignment see table 1.

Figure 3 Comparison of several recent MO-calculations for pyridine (Ref. 17-20). While most calculations agree on the grouping of the pyridine MO's into well seperated bunches they disagree concerning the individual ordering of MO's and in particular on the values for the binding energies for the low lying MO's ($E_B \geq 20$ eV).

Figure 4 Photoelectron energy distribution curves for $h\nu = 45$ eV for a clean silver surface (cross marked curve) and the silver/pyridine adsorbate system (upper panel). In the lower panel the difference spectrum (adsorbate minus Ag) is compared to the EDC of solid pyridine (see text).

Figure 5 Energy level diagram showing schematically the density of states N(E) for Ag and the filled orbitals of gaseous pyridine [16] as well as the MO scheme for pyridine on Ag obtained from photoemission experiments. The range of surface induced local 4d-states in the upper part of the Ag 4d band is indicated by the hatched area [22].

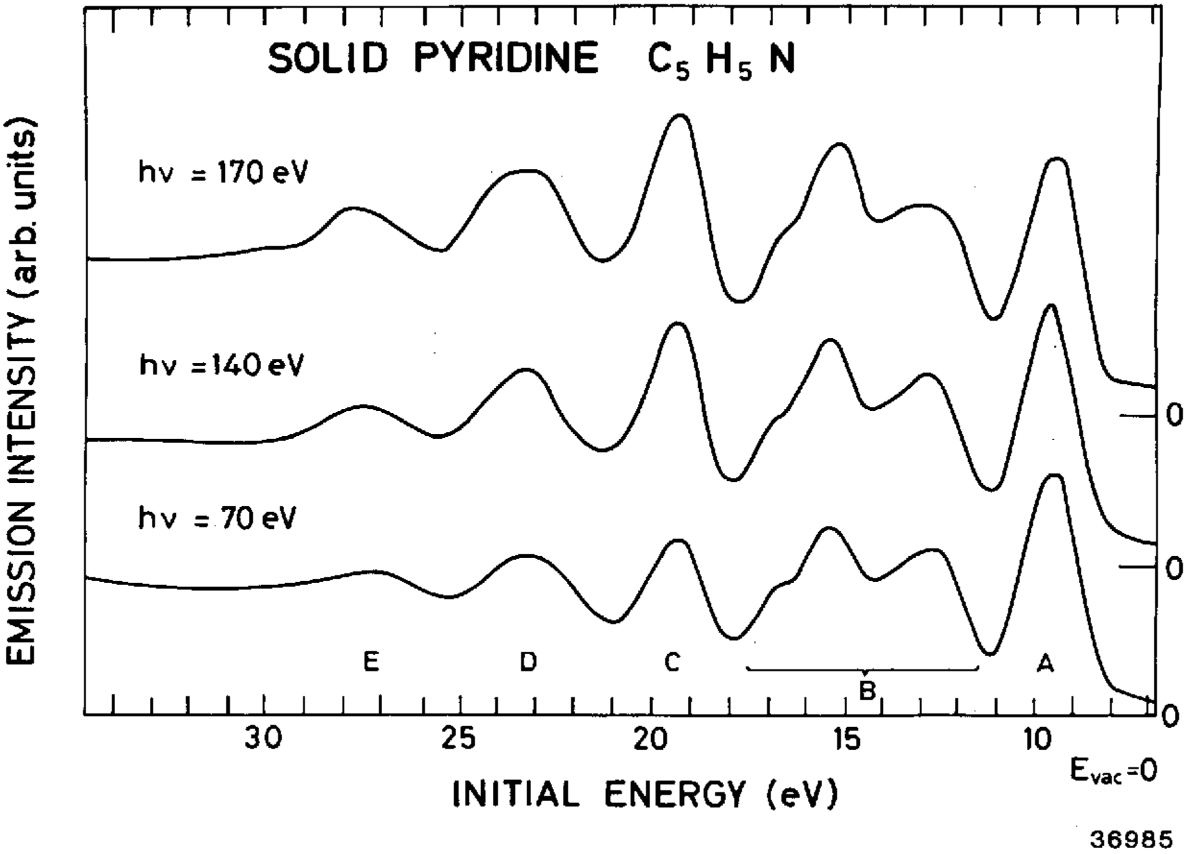
SOLID PYRIDINE C_5H_5N
EMISSION INTENSITY (arb. units)
hν = 170 eV
hν = 140 eV
hν = 70 eV
E
D
C
B
A
0
0
0
30
25
20
15
10
$E_{vac}=0$
INITIAL ENERGY (eV)
36985

Fig. 1

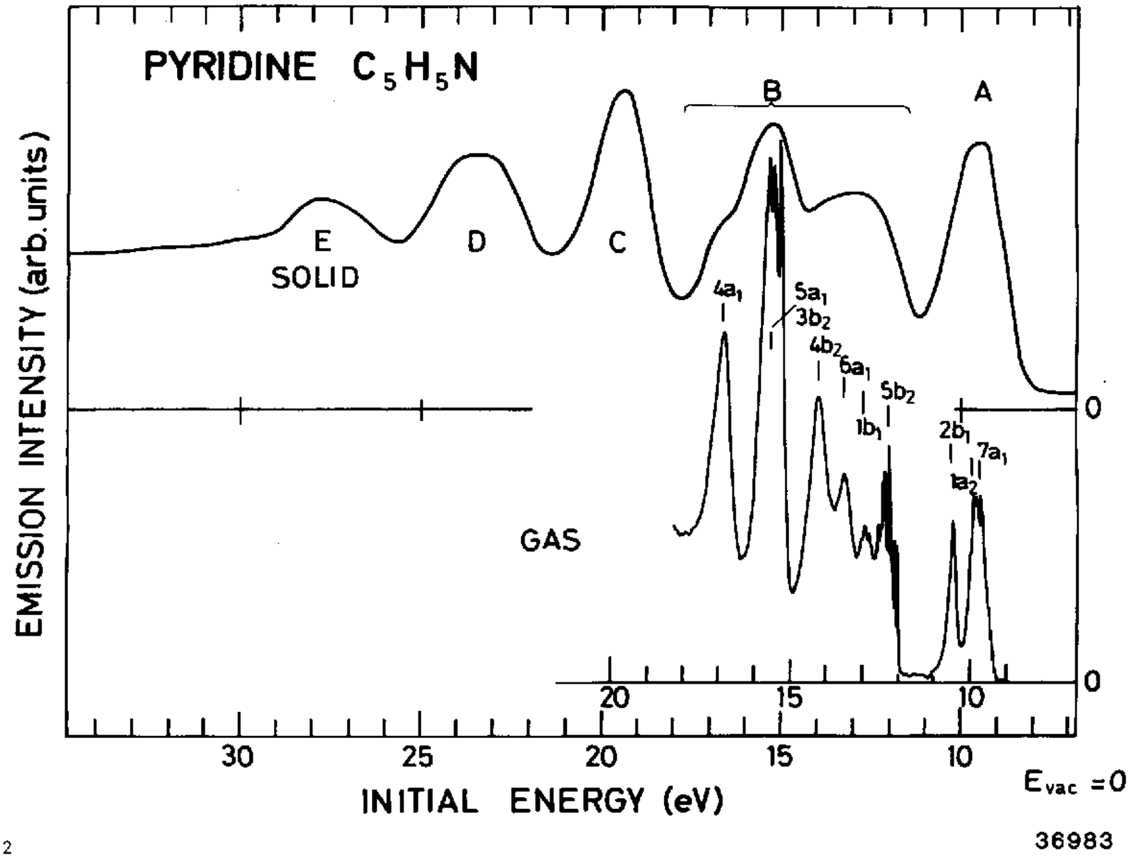
PYRIDINE C_5H_5N
EMISSION INTENSITY (arb. units)
B
A
E
D
C
SOLID
GAS
$4a_1$
$5a_1$
$3b_2$
$4b_2$
$6a_1$
$1b_1$
$5b_2$
$2b_1$
$7a_1$
$1a_2$
0
0
20
15
10
30
25
20
15
10
$E_{vac}=0$
INITIAL ENERGY (eV)
36983

Fig. 2

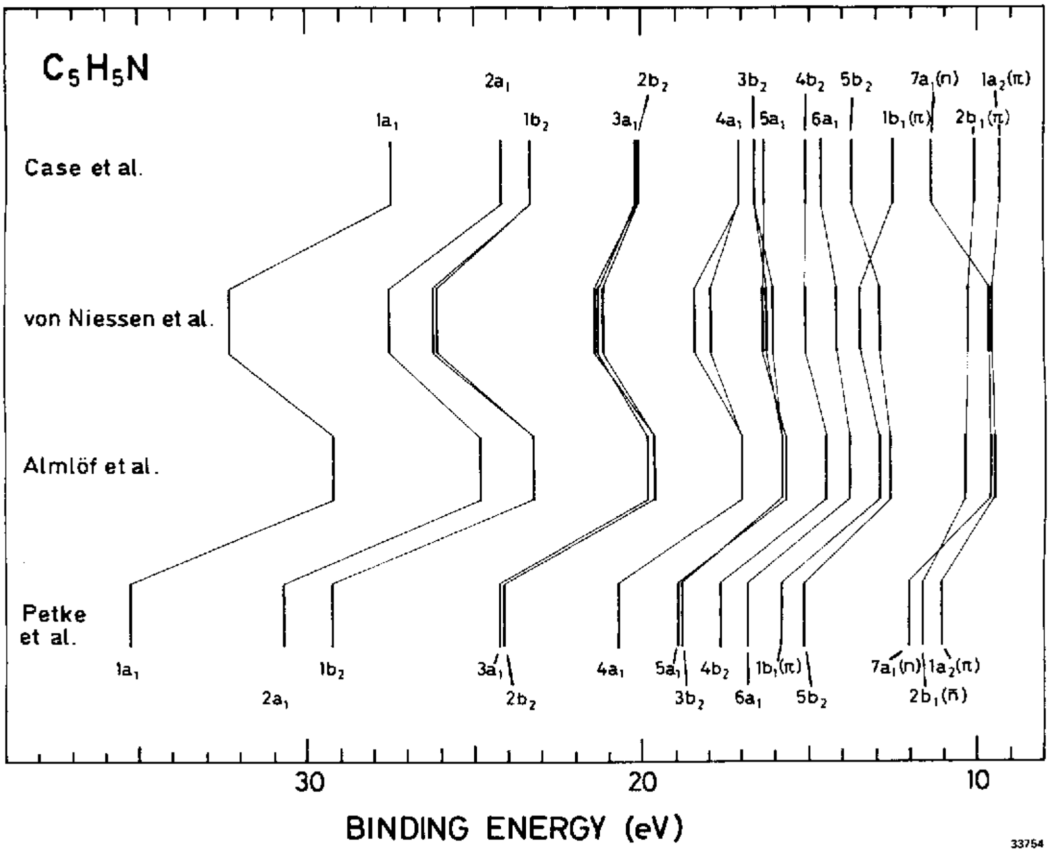
C_5H_5N
Case et al.
von Niessen et al.
Almlöf et al.
Petke et al.
$1a_1$
$2a_1$
$1b_2$
$3a_1$
$2b_2$
$4a_1$
$3b_2$
$5a_1$
$4b_2$
$6a_1$
$5b_2$
$1b_1(\pi)$
$7a_1(n)$
$2b_1(\pi)$
$1a_2(\pi)$
$2b_1(\bar{\pi})$
30
20
10
BINDING ENERGY (eV)
33754

Fig. 3

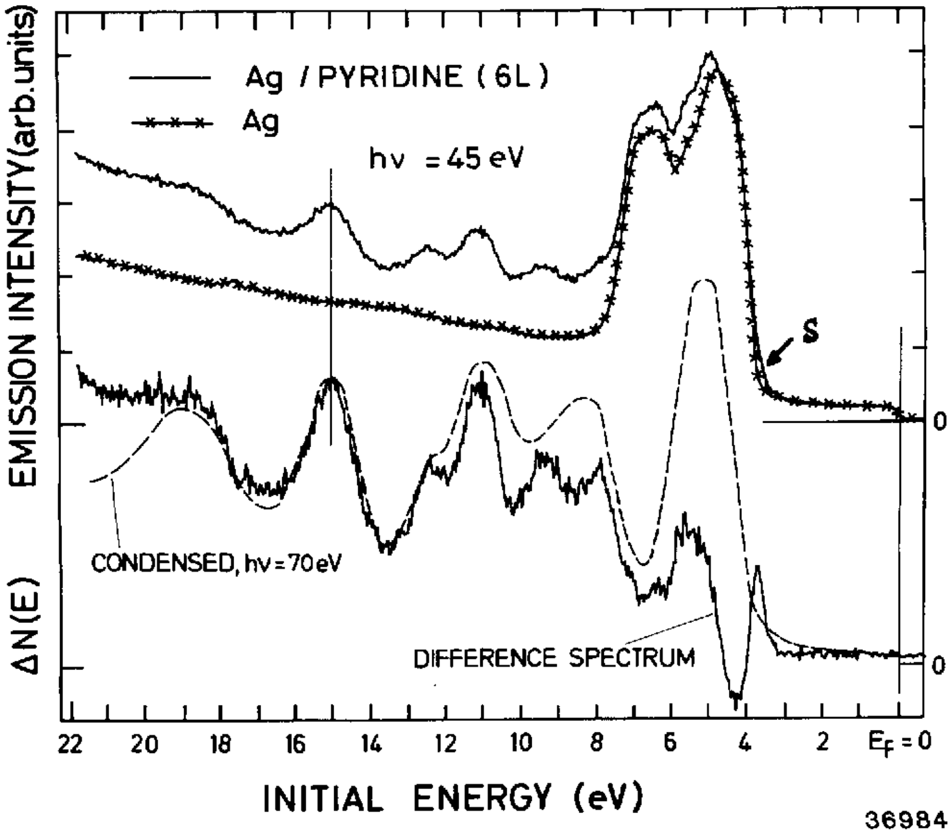
EMISSION INTENSITY(arb.units)
Ag / PYRIDINE (6L)
Ag
hν = 45 eV
S
0
CONDENSED, hν = 70 eV
ΔN(E)
DIFFERENCE SPECTRUM
0
22
20
18
16
14
12
10
8
6
4
2
$E_F = 0$
INITIAL ENERGY (eV)
36984

Fig. 4

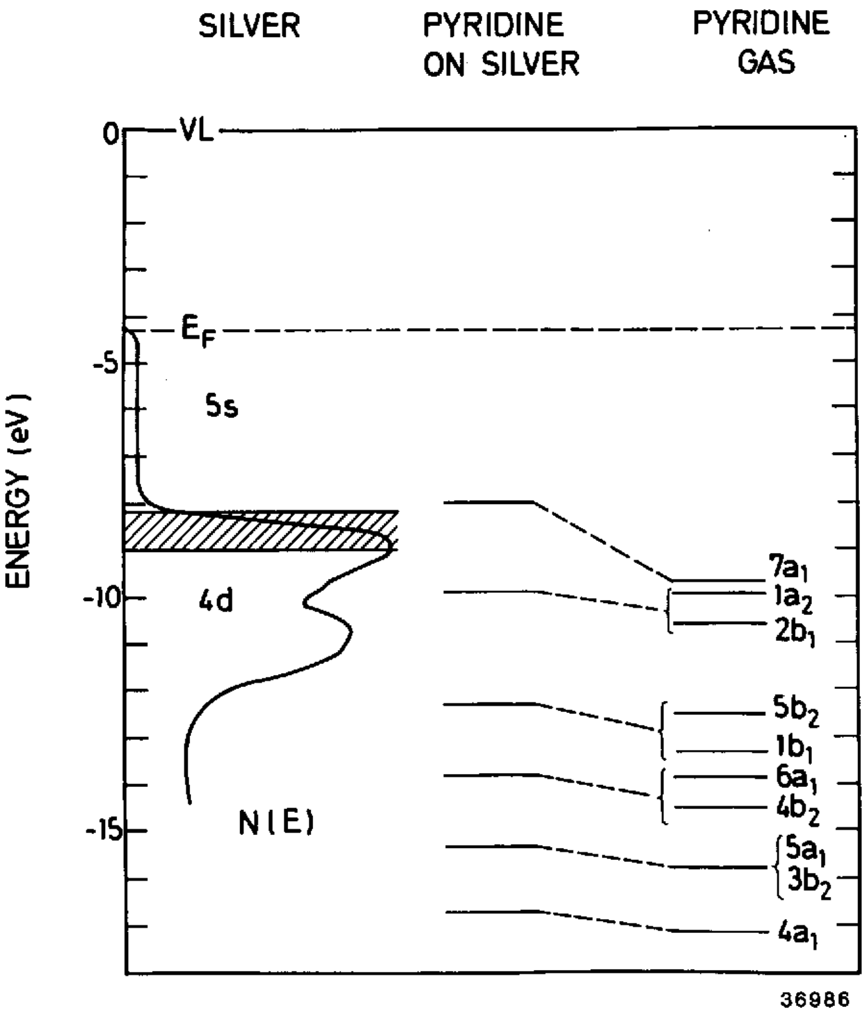
SILVER
PYRIDINE ON SILVER
PYRIDINE GAS
ENERGY (eV)
0
-5
-10
-15
VL
E_F
5s
4d
N(E)
$7a_1$
$1a_2$
$2b_1$
$5b_2$
$1b_1$
$6a_1$
$4b_2$
$5a_1$
$3b_2$
$4a_1$
36986

Fig. 5